Regular Article

The actin cortex as an active wetting layer

J.-F. Joanny[1], K. Kruse[2,a], J. Prost[1,3], and S. Ramaswamy[4,b]

[1] Physico Chimie Curie (Institut Curie, Cnrs UMR 168, UPMC), Institut Curie Centre de Recherche, 26 rue d'Ulm, 75248 Paris Cedex 05, France
[2] Theoretische Physik, Universität des Saarlandes, Postfach 151150, 66041 Saarbrücken, Germany
[3] ESPCI, 10 rue Vauquelin 75005 Paris, France
[4] TIFR Centre for Interdisciplinary Sciences, Tata Institute of Fundamental Research, 21 Brundavan Complex, Narsingi, Hyderabad 500 075 India

Abstract. Using active gel theory we study theoretically the properties of the cortical actin layer of animal cells. The cortical layer is described as a non-equilibrium wetting film on the cell membrane. The actin density is approximately constant in the layer and jumps to zero at its edge. The layer thickness is determined by the ratio of the polymerization velocity and the depolymerization rate of actin.

1 Introduction

Living cells maintain and change shape, adhere, spread, divide and crawl through the agency of a dynamic, filamentous scaffold known as the cytoskeleton [1]. Although this structure is made up of many different constituents the task of stress generation, with crucial consequences for the mechanical properties of cells, lies primarily with the *acto-myosin* component [2]. This substructure consists of a meshwork of semi-flexible actin filaments interacting with a large number of proteins among which myosin molecular motors play a major role. Myosin motors, assembled in minifilaments, consume free energy through the hydrolysis of ATP molecules and can produce work. By binding to the actin filaments, myosin minifilaments create contractile stresses in the actin gel.

The crosslinked polymer network formed by actin and its associated proteins differs profoundly from more familiar thermal-equilibrium physical or chemical gels because of the sustained energy dissipation by the molecular motors and some other proteins. It is usefully viewed as a state of active matter [3] known as an active polar gel [4–8] —"active" referring to the steady consumption of free energy at the scale of individual components, *i.e.*, the actin-bound molecular motors, and "polar" to the orientable, directed character of the actin filaments. In particular, each filament carries a distinction between its two extremities, as does each constituent monomer. We will therefore refer to the plus and the minus end of a filament.

The filaments of the cytoskeleton undergo constant assembly and disassembly: Each actin filament polymerizes preferentially at the plus end and depolymerizes at the minus end. This process is called treadmilling, and is regulated by a multitude of accessory proteins. Through depolymerization, filaments disintegrate, and through polymerization new filaments are generated, maintaining a non-zero gel mass on average. Generation of new filaments is assisted by nucleating proteins, such as formins that act as seeds for actin polymerization and then stay attached for some time to actin plus-ends, where they promote the addition of monomers. The Arp2/3 complex instead binds to existing filaments and remains attached to the minus end of newly created actin filaments.

In this work we study consequences of the interplay of actin polymerization and active contraction of actin gels through a hydrodynamic description, that captures the generic behavior of materials on large length and time scales. Such a description starts with the correct choice of slow variables [9] relying broadly on conservation laws, broken continuous symmetries, and order-parameter modes near a continuous phase transition. This approach has been successfully extended to active systems [3,4,10,11], held in stationary states far from thermal equilibrium by the sustained dissipation of free energy. Despite the very broad range of length scales, from microns to kilometers, on which organized active matter is seen, there is a degree of universality in its hydrodynamic properties, classified by the type of broken symmetry and applicable conservation laws: examples include waves without conventional inertia, anomalously large number fluctuations, and a tendency of instability of quiescent states towards spontaneous flow [3].

---

[a] e-mail: `k.kruse@physik.uni-saarland.de`
[b] On leave from Department of Physics, Indian Institute of Science, Bangalore 560 012, India.
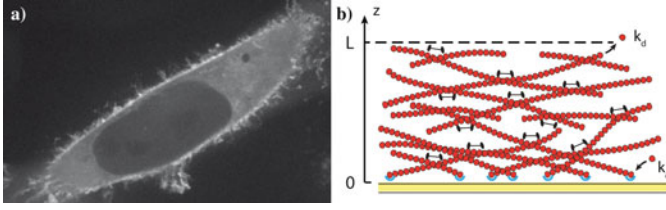
Fig. 1. a) Confocal fluorescence microscopy image of a HeLa cell with F-actin labeled by Lifeact-Ruby. Below the plasma membrane a well-defined zone of high fluorescence represents the actin cortex. Image with courtesy from M. Fritzsche and G. Charras. b) Schematic illustration of the cortex dynamics considered in this work. Nucleation-promoting factors located at the plasma membrane nucleate new actin filaments or assist elongation of existing filaments at rate k_a^*. This generates a flux of polymerized actin $v_p\rho_0$, where ρ_0 is the gel density at the surface and $v_p = k_a^*\delta$ is the polymerization velocity, δ being the size of an actin monomer. Filaments disassemble at a rate k_d anywhere in the cortex. Not shown is the growth of actin filaments away from the membrane. Molecular motors act as active cross-links and generate active stresses in the cortex.

We focus on the fact that a substantial fraction of the actomyosin is located in a layer, known as the actin cortex [12,13], adjacent to the plasma membrane of the cell, see fig. 1a. This localization of one component to the vicinity of a wall is reminiscent of the physical phenomenon of wetting. However, prevalent explanations of the cortical actin profile do not take advantage of this analogy, relying instead on an imposed spatial separation between the zones of polymerization and depolymerization. In this paper we show that the active contractility alluded to in an earlier paragraph can drive a transition to a steady state maintained by a polymerization-depolymerization process, see fig. 1b, in which the polymer concentration has a profile very similar to that of a wetting layer [14]. The cortex thickness and actin density profile emerge naturally from our treatment. Recall that in thermal equilibrium systems wetting arises through the selective attraction of a component to a surface. In the following we show that contractility, although quite different from an attractive potential, plays a similar role in driving a condensation at the plasma membrane. To obtain this result, we generalize the hydrodynamic description of active gels to include crucial non-linear density dependences.

The rest of this paper is organized as follows. In sect. 2 we present the hydrodynamic equations for polymerizing active gels. In sect. 3, we study an active gel polymerizing at a surface, which yields a description of the actin cortex of animal cells. The properties of the gel can be understood in terms of active wetting and dewetting by filament assembly and disassembly.

2 Hydrodynamic description

We now present the hydrodynamic equations governing the dynamics of an assembling active actin gel. We assume that the gel is assembled by actin polymerization at a sur-

face. In a cell or in an *in vitro* experiment, the polymerization is promoted by nucleating proteins, such as proteins of the formin family, see fig. 1b. Away from the surface, the actin gel assembles by elongation of existing filaments or by nucleation of new filaments. The gel disassembles because of monomer removal at filament minus-ends or by severing of the gel filaments that produces small filaments, which diffuse into the solution. Myosin molecular motors assemble into small filaments that act as cross-links, which actively generate mechanical stress in the filament network. The network is permeated by a solvent containing, in particular, unbound motors and actin monomers. We limit ourselves to the case where the exchange of motors between the actin network and the solvent is so fast that we can assume them to be equilibrated and where the motors diffusion is fast enough that the concentration of free motors in the solvent is constant. In a first approximation, the concentration of motors bound to actin is then proportional to the local actin concentration. We have verified numerically that our results do not change significantly when motor binding and unbinding and motor diffusion are taken explicitly into account, at least in the case when the gel does not impede the diffusion of motors.

As mentioned in the introduction, actin filaments are polar objects. Consequently, an actin gel can present a macroscopic vectorial order represented by a polarization field **p**. In the present treatment we ignore the subtleties associated with actin polarization and consider in the following the case of an isotropic gel. Our detailed calculations will be for the case where the actin concentration varies only along one direction, where transverse variations in **p** play no role.

Actin polymerizes on a planar surface located in the plane $z = 0$. The gel and the solvent are restricted to the half-space $z \geq 0$. If the gel is homogeneous in the directions parallel to the surface, its properties and in particular its density only depend on the z coordinate. We will explore elsewhere the dynamics of variations in the xy-plane.

2.1 Conservation laws

The hydrodynamic description is based on conservation laws for mass and momentum. Mass conservation of the gel and the solvent read

$$\partial_t\rho_{\mathrm{g}} + \partial_\alpha\rho_{\mathrm{g}}v_{\mathrm{g},\alpha} = -k_d\rho_{\mathrm{g}},$$
$$\partial_t\rho_{\mathrm{s}} + \partial_\alpha\rho_{\mathrm{s}}v_{\mathrm{s},\alpha} = k_d\rho_{\mathrm{g}}. \tag{1}$$

Greek indices denote the three spatial directions x, y, and z and we have adopted Einstein's summation convention.

In the above expressions, ρ_{g} and ρ_{s}, respectively, denote the densities of the gel and the solvent, while $\mathbf{v}_{\mathrm{g}}$ and $\mathbf{v}_{\mathrm{s}}$ are the corresponding velocities. Degradation of the gel due to depolymerization and severing occurs at a constant rate k_d. The gel is produced on the one hand by growth of existing filaments, and on the other hand by the nucleation of new actin filaments. There is no significant spontaneous nucleation of new filaments at concentrations of monomeric actin present in cells. Instead

nucleation-promoting factors regulate the generation of new filaments and their elongation. Members of the formin family and the Arp2/3 complex are important examples of nucleation-promoting factors [15–17]. Formin is located directly beneath the plasma membrane, where it generates new filaments. The Arp2/3 complex needs to bind to existing filaments before it can act as the seed of a new filament. Still, it is predominantly localized in the vicinity of the cell membrane. We therefore consider here for simplicity that the actin gel growth occurs only at the surface. Therefore, the filament density far away from the surface vanishes. We account for elongation and nucleation on the surface by a boundary condition on the gel flux at $z = 0$. Explicitly, we write $\rho_g v_{g,z}|_{z=0} = v_p \rho_0$, where v_p is the polymerization velocity and ρ_0 the gel density at the surface, which is imposed by the density of nucleation-promoting factors.

2.2 Constitutive relations

To fully specify the behavior of the actin gel, we must provide constitutive equations. They link the generalized thermodynamic fluxes to the generalized thermodynamic forces. We follow here closely the approach of Callan-Jones and Jülicher [18] to describe active permeating gels. The fluxes are in our case the gel velocity, the time derivative of the strain in the gel, the relative current between actin gel and solvent $\mathbf{j} = \rho_g(\mathbf{v}_g - \mathbf{v})$, where $\mathbf{v}$ is the center-of-mass velocity, the deviatoric stress tensor σ and the rate of ATP consumption. The generalized forces are the gradient in the relative chemical potential $\bar{\mu}$ of the gel and the solvent, the center-of-mass velocity gradient $\nabla \mathbf{v}$, the partial stress of the gel σ^g and the activity of the system. The relative chemical potential is given by $\bar{\mu} = \mu_g/m_g - \mu_s/m_s$, where μ_g and μ_s are the respective chemical potentials of the gel and the solvent and m_g and m_s the masses of the solvent and actin monomer molecules. Active processes are eventually driven by the hydrolysis of ATP into ADP and inorganic phosphate P_i, with chemical potentials μ_{ATP}, μ_{ADP}, and μ_P, respectively. We express the system's activity through the difference $\Delta\mu = \mu_{ATP} - \mu_{ADP} - \mu_P$. In the following $\Delta\mu$ is considered as constant in space and time. We do not consider any further the corresponding thermodynamic flux which provides the rate r of ATP consumption in the system.

The constitutive equations are obtained from an expansion of the thermodynamic fluxes in terms of the corresponding forces. Here, we give only the final equation for the relative current between actin and solvent for an isotropic active gel [18]

$$j_\alpha = -\gamma \partial_\alpha \bar{\mu} + \chi \partial_\beta \sigma^g_{\alpha\beta}. \qquad (2)$$

In this expression $\sigma^g_{\alpha\beta}$ are the components of the partial stress tensor of the gel phase, not to be confused with the total stress [18]. It is analogous to the particle phase stress in suspension mechanics [19,20] In steady state, elastic effects vanish and the stress is purely viscous, so that $\sigma^g_{\alpha\beta} = 2\eta v_{g,\alpha\beta} - \zeta \Delta\mu \delta_{\alpha\beta}$ where η is the gel viscosity,

$v_{g,\alpha\beta} = \frac{1}{2}(\partial_\alpha v_{g,\beta} + \partial_\beta v_{g,\alpha})$, and $\zeta\Delta\mu$ gives the magnitude of the actively generated (isotropic) stress in the gel phase. The first term in expression (2) accounts for the diffusive current due to gradients in the relative chemical potential. The second term describes the flux that results from gradients in the gel stress. Finally, the permeation constant $\rho_g \chi^{-1} \sim \eta_s/\xi^2$, where ξ is the gel's mesh size and η_s the solvent viscosity.

As the only vector for a non-polar system is the gradient vector, within the Onsager linear approach the active contribution to the current is proportional to $\partial_\alpha \Delta\mu$ and vanishes if $\Delta\mu$ is constant in space, which we assume. Fluxes stemming from the system's activity are captured by the last term of the stress expression. The coupling parameter ζ here depends on the gel density ρ_g and is negative due to the contractility of the motors.

We proceed using the same approximation as in ref. [18]: The osmotic pressure $\tilde{\Pi}$ satisfies the Gibbs-Duhem equation $d\tilde{\Pi} = \rho_g d\mu$, if the volume of the system is independent of the composition and incompressible. We define an effective osmotic pressure including active effects as $\Pi = \tilde{\Pi} + \zeta\Delta\mu$ and, we thus get

$$\frac{\rho_g}{\chi}(v_{g,\alpha} - v_\alpha) = 2\eta \partial_\beta v_{g,\alpha\beta} - \partial_\alpha \Pi, \qquad (3)$$

where we have expressed the gel stress in terms of the gel shear rate. There are two competing dissipative mechanisms, the gel viscosity and permeation of the solvent through the actin gel. The comparison between these two types of dissipation defines a permeation length $L_p = (\eta \rho_g^{-1} \chi)^{1/2} \sim (\eta/\eta_s)^{1/2}\xi$. The relative permeation current on the left-hand side of eq. (3) is negligible compared to the viscous dissipation term if we consider the dynamics on length scales smaller than the permeation length scale L_p. For typical viscosities $\eta \sim 10^8 \eta_s$ and typical mesh sizes of ξ of a few tens of nanometers, the characteristic length is of the order of a few hundreds of microns and thus macroscopic. We therefore neglect permeation in the following.

From now on, we consider only the gel density ρ_g and the corresponding velocity field v_g. Dropping the g indices, the equations read

$$\partial_t \rho + \partial_\alpha \rho v_\alpha = -k_d \rho,$$
$$2\eta \partial_\beta v_{\alpha\beta} - \partial_\alpha \Pi(\rho) = 0. \qquad (4)$$

These equations are identical to those of a hydrodynamic theory for an effective one component compressible active gel [4,5].

3 Active pre-wetting

We consider a situation where the gel is assembling at the surface located at $z = 0$ and assume invariance under translations in the surface plane. This leaves us with a one-dimensional problem. The dynamic equations (4) read for $z \geq 0$

$$\partial_t \rho + \partial_z \rho v = -k_d \rho,$$
$$2\eta \partial_z v - \Pi(\rho) = 0, \qquad (5)$$

where v denotes the z-component of the gel velocity. The second equation follows from integrating eq. (4). Let us recall that the boundary condition on the gel current at the surface is $\rho v|_{z=0} = \rho_0 v_p$.

To complete our description, we need to provide an expression for the effective pressure Π. Usually, the osmotic pressure $\tilde{\Pi}$ is a monotonic increasing function of the actin density. However, the active contribution is negative and has a maximum as a function of density for a given crosslink density [21]. The passive osmotic pressure always dominates at large densities but if activity is large enough, the effective osmotic pressure can become a non-monotonic function of density, which is indicative of a phase separation in the solution induced by the contractility of the molecular motors. In the following, we use

$$\Pi = a\rho^3 + b\rho^4, \qquad (6)$$

where the coefficient a depends on activity. For vanishing activity, standard three-body interactions should dominate and a should be positive. For large activity, contractility should dominate and a should be negative. In principle, the expansion in powers of ρ should contain linear and quadratic terms as well. Whether contractility should be reflected in the quadratic or in the cubic term depends on how the motor density relates to the actin polymeric density. For example, one could argue that contractility requires a pair of actin filaments as well as myosin, so if the bound myosin concentration is proportional to that of the filamentous actin, one would expect a cubic ρ dependence. The choice of the functional form is not essential, what really matters is the non-monotonicity of $\Pi(\rho)$. If $a < 0$ then the activity leads to contractile stresses.

We solve eq. (5) in steady state. Combining the two equations, we get for the velocity field

$$2\eta v = \left(\frac{\partial \rho}{\partial z}\right)^{-1} \rho f(\rho), \qquad (7)$$

where we have introduced the auxiliary function

$$f(\rho) = -2k_d\eta - a\rho^3 - b\rho^4. \qquad (8)$$

The general solution to the steady state equations can then be written in the form

$$\frac{\mathrm{d}\rho}{\mathrm{d}z} = \frac{1}{2\rho_0\eta v_p}\rho^2 f(\rho) \exp\left\{\int_{\rho_0}^{\rho} \frac{2k_d\eta}{\rho' f(\rho')}\mathrm{d}\rho'\right\}, \qquad (9)$$

leading to

$$v = \frac{\rho_0}{\rho}v_p \exp\left\{-\int_{\rho_0}^{\rho} \frac{2k_d\eta}{\rho' f(\rho')}\mathrm{d}\rho'\right\}. \qquad (10)$$

From these solutions we infer that the gel density ρ jumps to zero at densities fulfilling $f(\rho) = 0$. Indeed, equation (10) implies $v \geq 0$ with $v = 0$ for $f = 0$ and no material is transported beyond such a point. Consequently, as soon as f presents zeros a well-defined cortical layer with a sharp edge can be formed. The existence of zeros of f depends on the activity. There exists a critical value a_c

beyond which a wetting layer appears. For $-a > -a_c > 0$ the function has two zeros, while for $-a < -a_c$ it has none. If the activity is equal to the critical value a_c, the function f has exactly one zero. As we will discuss below, the transition at $a = a_c$ can be viewed as an active or non-equilibrium analog of a pre-wetting transition [14,22].

3.1 The weak contractile activity regime

The weak contractile activity regime is defined by $-a < -a_c$, such that $f(\rho) < 0$ for all ρ. Since ρ tends to zero as $z \to \infty$, we have in this case $f(\rho) \approx -2k_d\eta$ and thus

$$\frac{\mathrm{d}\rho}{\mathrm{d}z} \approx -\frac{k_d}{\rho_0 v_p}\rho^2 \exp\left\{-\ln\frac{\rho}{\rho_0'}\right\}, \qquad (11)$$

where ρ_0' is a constant. The density thus eventually decays exponentially. If ρ_0 is small, we have $\rho_0' \approx \rho_0$ and

$$\frac{\mathrm{d}\rho}{\mathrm{d}z} = -\frac{k_d}{v_p}\rho, \qquad (12)$$

such that the characteristic length is v_p/k_d. For large values of ρ_0, the characteristic length is instead $v_p\rho_0/k_d\rho_0'$, with

$$\rho_0' = \rho_0 \exp\left\{\int_0^{\rho_0} \frac{2k_d\eta}{\rho'}\left(\frac{1}{f(\rho')} + \frac{1}{2k_d\eta}\right)\mathrm{d}\rho'\right\}. \qquad (13)$$

The profile can thus be a simple exponential or it can present a "shoulder" presaging the existence of a well-defined cortical layer for high contractile activity. In the latter case, the profile presents two inflection points, which are determined by $\partial(\partial_z\rho)/\partial\rho = \infty$. This equation has two solutions for $-a$ large enough but still smaller than $-a_c$. In this case, we can define the layer thickness L via the condition of mass conservation in steady state $\rho_0 v_p \sim k_d\rho_m L$, where ρ_m is approximately given by the value of ρ maximizing f.

Examples of density profiles for a subcritical activity and two different values of ρ_0 are given in fig. 2.

3.2 The large contractile activity regime

We consider now the case $-a > -a_c$, such that $f(\rho)$ has two real roots $\rho_1 > \rho_2$. From eq. (7) and since $v \geq 0$, we infer that for a density $\rho(z = 0) = \rho_0 < \rho_2$ the density approaches 0 with increasing z. Indeed, in this case $\partial\rho/\partial z < 0$ for all $z > 0$. As a consequence, the density profile behaves very similarly to the weak activity case $-a < -a_c$. In contrast, for $\rho_0 > \rho_2$, the density approaches the value ρ_1. As $v \to 0$ for $\rho \to \rho_1$, this value is reached at a finite distance z from the surface.

We can calculate the density profile for $\rho \approx \rho_1$. Then $f(\rho) = -\alpha(\rho - \rho_1)$ with $\alpha = |f'(\rho_1)|$ such that

$$\int_{\rho_0}^{\rho} \frac{2k_d\eta}{\rho' f(\rho')}\mathrm{d}\rho' \approx -\frac{2k_d\eta}{\alpha\rho_1}\ln\frac{|\rho - \rho_1|}{|\rho_0 - \rho_1|} \qquad (14)$$
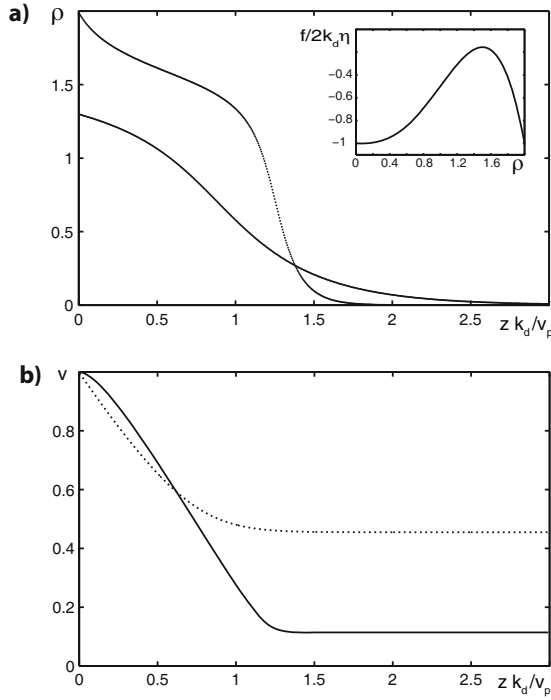
Fig. 2. Steady state density and velocity profiles in the weakly active regime, $-a < -a_c$ from numerical solutions of eqs. (5). a) Densities as a function of the distance from the polymerizing surface for surface densities $\rho_0 = 1.3$ and $\rho_0 = 2.0$, respectively. Inset: auxiliary function $f(\rho)$. b) Corresponding velocity profiles; dotted: $\rho_0 = 1.3$ and solid: $\rho_0 = 2.0$. Parameters are $a = -2k_d\eta$ and $b = k_d\eta$.

and

$$\frac{d\rho}{dz} = -\frac{\alpha\rho_1^2}{2\rho_0\eta v_p}(\rho - \rho_1)\left[\frac{|\rho - \rho_1|}{|\rho_0 - \rho_1|}\right]^{-2k_d\eta/\alpha\rho_1}. \quad (15)$$

We can solve the latter equation explicitly. In the case $\rho_0 \approx \rho_1$ we get for the whole density profile

$$\rho(z) = \rho_1 + (\rho_0 - \rho_1)\left\{\frac{\rho_1}{\rho_0}\frac{k_d}{v_p}(L - z)\right\}^{\alpha\rho_1/2k_d\eta}. \quad (16)$$

Note, that the density profile in the vicinity of L depends on the value of $\alpha\rho_1/2k_d\eta$ that fixes the slope of the profile when $\rho = \rho_1$. In figs. 3 and 4, we present steady state solutions for various nucleator densities ρ_0 for $\alpha\rho_1/2k_d\eta < 1$ and $\alpha\rho_1/2k_d\eta > 1$, respectively.

The thickness of the gel layer is given by the flux balance condition $\rho_0 v_p = \int_0^L k_d\rho\,dz$. Alternatively, we can estimate the cortex thickness by setting $z = 0$ in the approximate density profile (16), yielding

$$L \sim \frac{\rho_0}{\rho_1}\frac{v_p}{k_d}. \quad (17)$$

As can be seen in figs. 3 and 4, for $\rho \approx \rho_0$ it approximates well the thickness obtained from the numerical solution to eqs. (5). For $\rho_0 > \rho_1$ the length increases linearly with ρ_0, however, with a slope that is different from the one given in eq. (17).
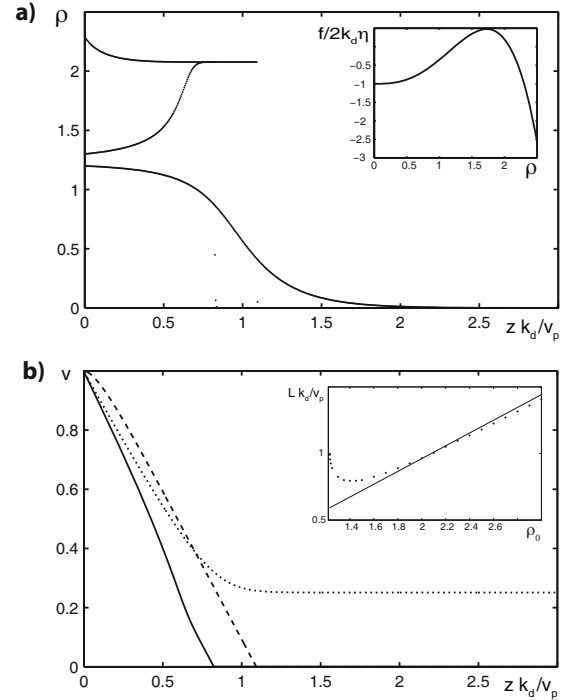

Fig. 3. Steady-state density and velocity profiles in the strongly active regime, $-a > -a_c$, from numerical solutions of eqs. (5). a) Densities as a function of the distance from the polymerizing surface for surface densities $\rho_0 = 1.2$, $\rho_0 = 1.3$, and $\rho_0 = 2.3$, respectively. Inset: auxiliary function $f(\rho)$, which has zeros at $\rho_1 = 2.08$ and $\rho_2 = 1.23$. b) Corresponding velocity profiles; dotted: $\rho_0 = 1.2$, solid: $\rho_0 = 1.3$, and dashed: $\rho_0 = 2.3$. Inset: cortex width as a function of ρ_0 from numerical solution of eqs. (5) (dots) and from eq. (17) (line). Parameters are $a = -2.3k_d\eta$ and $b = k_d\eta$.

4 Discussion

In this work, we have introduced a hydrodynamic theory for describing the dynamics of active gels in the presence of filament polymerization and depolymerization. Our description of filament assembly and disassembly requires some comments. Specifically, we have taken the depolymerization rate and viscosity to be constant. Our main results are more general and do not depend on this assumption. The same behavior is obtained if we keep the gel density dependences of depolymerization rate and viscosity. In general, however, the depolymerization process is more complex as the rate of filament disassembly depends on mechanical stresses, the degree of severing, and the presence of actin-associated proteins like cofilin or gelsolin. In addition the fact that filaments depolymerize from their ends might introduce a gradient in the effective depolymerization rate. Together these processes might even lead to filament subpopulations with different turnover rates [23]. Similarly, the polymerization process is more involved than assumed in the present work. We have restricted it to be spatially localized at the membrane, while actin filaments also grow in the bulk and can be nucleated away from the membrane. This possibility will be discussed in a forthcoming publication. We be-
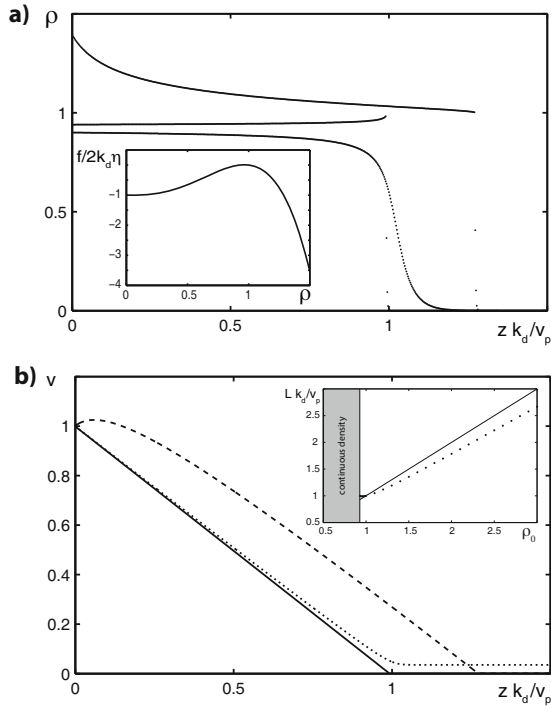
Fig. 4. Steady state density and velocity profiles in the strongly active regime, $-a > -a_c$, from numerical solutions of eqs. (5). a) Densities as a function of the distance from the polymerizing surface for surface densities $\rho_0 = 0.9$, $\rho_0 = 0.94$, and $\rho_0 = 1.4$, respectively. Inset: auxiliary function $f(\rho)$, which has zeros at $\rho_1 = 1.0$ and $\rho_2 = 0.93$. b) Corresponding velocity profiles; dotted: $\rho_0 = 0.9$, solid: $\rho_0 = 0.94$, and dashed: $\rho_0 = 1.4$. Inset: cortex width as a function of ρ_0 from numerical solution of eqs. (5) (dots) and from eq. (17) (line). Parameters are $a = -9k_d\eta$ and $b = 7k_d\eta$.

lieve, however, that linking cortex formation to an out-of-equilibrium wetting phenomenon opens a new way of thinking about the problem worth being fully investigated. This picture is a non-equilibrium analog of a (pre-)wetting transition whereby the actin condensation on the membrane is driven by the contractility of the myosin molecular motors. For sufficiently strong motor activity, the actin density is almost constant up to a certain thickness, where it drops sharply to zero. Our simplified theory produces a singularity at the edge of the layer. This singularity can be smoothed out by adding terms in the osmotic pressure depending on the gradient of the density as is classically done in Ginzburg-Landau theory. The thickness of the non-equilibrium wetting layer is determined by the polymerization velocity at the membrane and the depolymerization rate.

The description of the cortical actin layer as an active wetting layer suggests several extensions of this work. The interaction between two adjacent cortical layers is obviously important in situations when the cell thickness becomes small. This is notably the case for the lamellipodia of cells crawling on a solid substrate, for example, keratocyte cells. Under these conditions one might expect a non-equilibrium analog of capillary condensation [24,25].

While in this work we have focused on steady-state properties of the cortical layer, we have also started to study the dynamics of cortex formation as well as dynamic instabilities of the cortex. In addition, our theory can be applied to *in vitro* experiments on cell extracts that contract in presence of actin assembly and disassembly [21].

References

1. B. Alberts *et al.*, *Molecular Biology of the Cell*, 5th edition (Garland Sci., Abbingdon, UK, 2008).
2. J. Howard, *Mechanics of Motor Proteins and the Cytoskeleton* (Sinauer Associates, Inc., Sunderland, 2001).
3. M.C. Marchetti *et al.*, to be published in Rev. Mod. Phys. (arXiv: 1207.2929).
4. K. Kruse, J.-F. Joanny, F. Jülicher, J. Prost, K. Sekimoto, Phys. Rev. Lett. **92**, 078101 (2004).
5. K. Kruse, J.-F. Joanny, F. Jülicher, J. Prost, K. Sekimoto, Eur. Phys. J. E **16**, 5 (2005).
6. J.-F. Joanny, F. Jülicher, K. Kruse, J. Prost, New J. Phys. **9**, 422 (2007).
7. Y. Hatwalne, S. Ramaswamy, M. Rao, R.A. Simha, Phys. Rev. Lett. **92**, 118101 (2004).
8. F. Jülicher, K. Kruse, J. Prost, J.-F. Joanny, Phys. Rep. **449**, 3 (2007).
9. P.C. Martin, O. Parodi, P.S. Pershan, Phys. Rev. A **6**, 2401 (1972).
10. J. Toner, Y. Tu, Phys. Rev. E **58**, 4828 (1998).
11. R.A. Simha, S. Ramaswamy, Phys. Rev. Lett. **89**, 058101 (2002).
12. G. Salbreux, J.-F. Joanny, J. Prost, P. Pullarkat, Phys. Biol. **4**, 268 (2007).
13. O. Medalia *et al.*, Science **298**, 1208 (2002).
14. J.W. Cahn, J. Chem. Phys. **66**, 3677 (1977).
15. S. Romero *et al.*, Cell **119**, 419 (2004).
16. B. Bugyi, M.-F. Carlier, Annu. Rev. Biophys. **39**, 449 (2010).
17. V. Achard *et al.*, Curr. Biol. **20**, 423 (2010).
18. A.C. Callan-Jones, F. Jülicher, New J. Phys. **13**, 093027 (2011).
19. G.K. Batchelor, J. Fluid Mech. **41**, 545 (1970).
20. P.R. Nott, J.F. Brady, J. Fluid Mech. **275**, 157 (1994).
21. P.M. Bendix *et al.*, Biophys. J. **94**, 3126 (2008).
22. E. Brézin, B. Halperin, S. Leibler, Phys. Rev. Lett. **50**, 1387 (1983).
23. M. Fritzsche, A. Lawalle, T. Duke, K. Kruse, G. Charras, Mol. Biol. Cell. **24**, 757 (2013).
24. J.S. Rowlinson, B. Widom, *Molecular Theory of Capillarity* (Oxford University Press, Oxford, 1989).
25. F. Restagno, L. Bocquet, T. Biben, Phys. Rev. Lett. **84**, 2433 (2000).